Orthogonally polarized bright–dark pulse pair generation in mode-locked fiber laser with a large-angle tilted fiber grating

Zuxing Zhang [1, 2, †], Chengbo Mou [2], Zhijun Yan [2], Zhongyuan Sun [2], Lin Zhang [2]

[1] School of Optoelectronic Engineering, Nanjing University of Posts and Telecommunications, Nanjing 210003, China

[2] Aston Institute of Photonic Technologies, Aston University, Birmingham B4 7ET, UK

E-mail: [†]zxzhang@njupt.edu.cn

Abstract: We report on the generation of orthogonally polarized bright–dark pulse pair in a passively mode-locked fiber laser with a large-angle tilted fiber grating (LA-TFG). The unique polarization properties of the LA-TFG, i.e. polarization-dependent loss and polarization-mode splitting, enable dual-wavelength mode-locking operation. Besides dual-wavelength bright pulses with uniform polarization at two different wavelengths, the bright–dark pulse pair has also been achieved. It is found that the bright–dark pulse pair is formed due to the nonlinear couplings between lights with two orthogonal polarizations and two different wavelengths. Furthermore, harmonic mode-locking of bright–dark pulse pair has been observed. The obtained bright–dark pulse pair could find potential use in secure communication system. It also paves the way to manipulate the generation of dark pulse in terms of wavelength and polarization, using specially designed fiber grating for mode-locking.

1. Introduction

In addition to having enormously broad impact as sources of ultrashort pulses [1], mode-locked fiber lasers exhibit complex nonlinear dynamics [2, 3], and are powerful tools for investigating the pulse evolutions in nonlinear systems. Two classes of pulses in fiber lasers have been identified: bright pulse, which is a sharp increment of laser intensity beyond a continuous laser background, and dark pulse, which is, in contrast, a deep intensity dip below a continuous laser background with nonzero intensity. The dark pulses are less sensitive to noise and fiber losses than the bright ones and hence are promising for robust optical communication [4]. Since the dark soliton transmission was first theoretically proposed in 1973 [5], the dark soliton formation and propagation in single-mode fibers (SMFs) has been extensively investigated on both theory and experiment [6-10]. It has been theoretically shown that both bright and dark solitons are solutions of the nonlinear Schrödinger equation (NLSE) [11], and can be supported in a fiber transmission line with dispersion management [12]. Quiroga-Teixeiro et al. [13] theoretically investigated and predicted the formation of a dark soliton in a mode-locked fiber laser by dissipative four-wave

mixing.

To date, there have been many demonstrations of dark pulse generation. Dark soliton formation, an intrinsic feature of the nonlinear light propagation in the normal dispersion fibers with balance between the fiber dispersion and nonlinearity, was first experimentally observed by Emplit et al. [14]. Relied on dissipative four-wave mixing method, the generation of dark soliton train in a self-induced modulation instability laser was experimentally demonstrated by Sylvestre et al. [15]. Then, Zhang et al. realized dark solitons in an all-normal dispersion fiber ring laser using the nonlinear polarization rotation (NPR) technique [16]. Taking advantage of the modulation instability induced in a fiber loop cavity, the dark soliton fiber laser with repetition rates increased as high as 280 GHz has recently been demonstrated [17].

Due to the interaction between the pulses, in addition to obtaining bright or dark pulses in fiber lasers, bright-bright, dark-dark, or bright-dark soliton pairs, as stationary solutions of coupled higher-order NLSE in fiber systems [18, 19], may coexist when they propagate together in the medium [20]. Especially, bright-dark soliton pairs have potential applications in secure communication system, in which the bright-dark soliton pair can be used to form security codes [21]. The generation of bright–dark pulse pair in a figure-eight dispersion managed (DM) passively mode-locked fiber laser with net anomalous cavity group velocity dispersion (GVD) has recently been reported [22]. The nonlinear amplifying loop mirror (NALM) is employed in this configuration to allow for passively mode-locked operation. However, due to the absence of wavelength selection, the dark solitons were randomly formed and uncontrolled.

In this Letter, we report the generation of bright–dark pulse pair in a passively mode-locked fiber laser with an LA-TFG. The polarization-dependent LA-TFG can be utilized as an in-fiber polarizer for mode-locking, and simultaneously as a two-wavelength filter resulted from polarization-mode splitting. The obtained dual-wavelength bright pulses have the same polarization at two different wavelengths, while the bright–dark pulse pair formed due to the nonlinear coupling between the bright and dark pulses exhibit orthogonal polarization at two different wavelengths. Using LA-TFG specially designed in terms of wavelength and polarization for mode-locking paves the way to manipulate the generation of dark pulse. The achieved bright–dark pulse pair has potential application value in secure communication system.

2. Experiment setup and results

The schematic of the mode-locked erbium-doped fiber laser with an LA-TFG is shown in Fig. 1. The laser consists of 1 m erbium-doped fiber (EDF) with nominal absorption coefficient of ~80 dB/m at 1530 nm and normal dispersion β^2=66.1 ps^2/km. The EDF is pumped through a 980/1550 wavelength division multiplexing (WDM) from a grating stabilized 975 nm laser diode (LD), which can provide up to 600 mW pump power. A polarization-independent optical isolator is used to ensure single direction oscillation. An LA-TFG is employed to induce polarization-dependent loss and polarization spectrum filtering for both mode-locking and wavelength selection. Two in-fiber polarization controllers (PC1and PC2) are located before and after the LA-TFG. A 10:90 fiber coupler is placed after the EDF to tap 10% of laser power out of the cavity. In order to achieve

mode-locking, a length of 150-m dispersion-shifted fiber (DSF) is incorporated into the cavity to increase the nonlinear effect. The DSF has a dispersion coefficient of -5 ps^2/km. Thus, the total cavity length is ~153.7 m, and the cavity net dispersion is ~-0.75 ps^2. The pulse spectrum and the output pulse train are investigated with an optical spectrum analyzer and an oscilloscope, respectively.
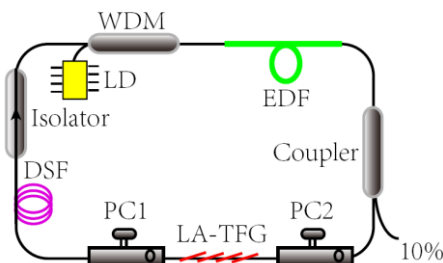

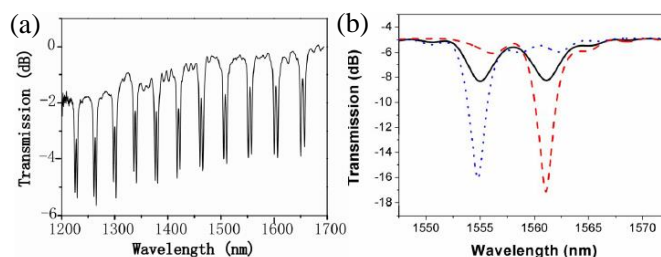**Figure 1** Schematic of mode-locked fiber laser with an LA-TFG.

Figure 2 Measured transmission of the LA-TFG (a) from 1200 nm to 1700 nm range and (b) from 1548 nm to 1572 nm range under different polarization excitation.

45^0-tilted fiber grating has been proposed to be used as in-fiber polarizer for mode-locking [23, 24]. LA-TFG, which is a type of tilted grating with tilted angle larger than 45^0, has been employed previously as fiber sensors for strain, twist, loading, refractive index (RI) and liquid level [25-29]. Our used LA-TFG was inscribed in H_2-loaded standard telecom fiber (SMF-28) by use of a frequency-doubled Ar^+ laser and the scanning mask technique. A commercial amplitude mask (from Edmund Optics Ltd) with a period of 6.6 μm was utilized for the LA-TFG inscription. During the inscription process, the amplitude mask was tilted at ~73^0 to induce in-fiber fringes blazed at ~78^0. The typical measured transmission spectrum of an LA-TFG shows a series of dual-peak resonances in the wavelength range from 1200 nm to 1700 nm with a nearly even separation between adjacent resonances [30], as shown in Fig. 2(a). The zoomed one paired peaks at wavelength of 1554.9 nm and 1561 nm is shown in Fig. 2(b). When the light is polarized, either the equivalent fast- or the slow-axis mode can be fully excited or eliminated. The blue dotted line indicates the fast-axis mode, while the dashed red line shows the slow-axis mode. The full strength of the loss peak reached ~10 dB when it was fully excited. The black solid curve illustrates excitation of the two modes with un-polarized light. It can be seen that the fabricated LA-TFG features polarization-dependence and polarization-mode splitting.
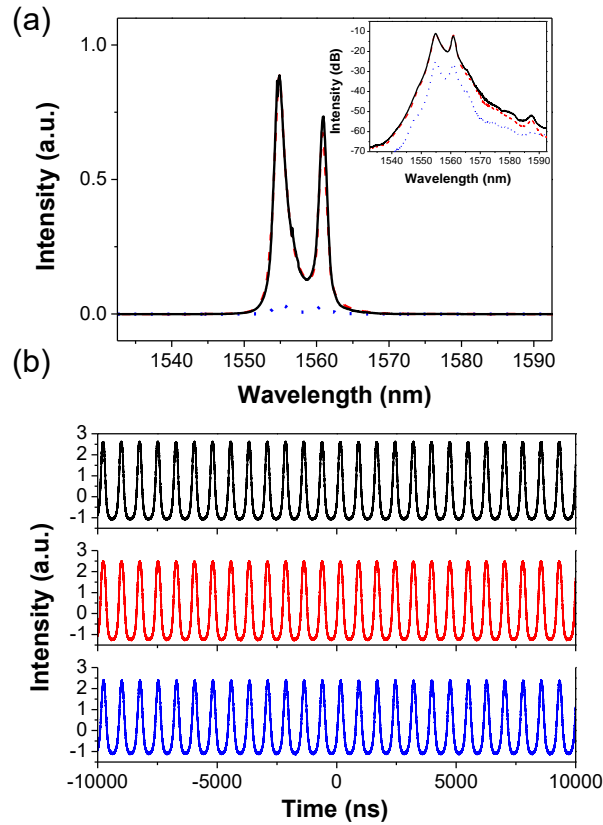
Figure 3 (a) Spectrum of dual-wavelength bright pulse (black solid line) and its polarization-resolved spectra (red dashed and blue dotted lines) on linear scale (inset is on logarithmic scale), (b) corresponding oscilloscope traces (red and blue lines).

In the experiment, in addition to single-wavelength mode-locked pulses, the stable dual-wavelength bright pulses with the fundamental repetition rate can be easily observed through appropriately adjusting the PCs, when the pump power is increased to the mode-locking threshold of about 178 mW. The optical spectrum of the dual-wavelength mode-locked bright pulses at 180 mW pump power is shown in Fig. 3(a). The dual-wavelength pulse simultaneously oscillates at 1554.8 and 1560.9 nm. The profile of dual-wavelength mode-locking pulse exhibits rectangular shape on the oscilloscope trace, as shown in Fig. 3(b). The pulse repetition rate is 1.32 MHz. To validate simultaneous mode-locking at two wavelengths, a tunable filter with maximal 3-dB bandwidth of 0.95 nm was utilized to separate the laser emissions. It is shown that rectangular pulse mode-locking operation exists at each wavelength. The rectangular pulse generation is a result of the accumulation of nonlinear effect and the clamp of peak power in the passively mode-locked fiber laser [31]. Furthermore, to investigate the polarization characteristics of the dual-wavelength bright pulse, another PC and a polarization beam splitter (PBS) at the output end were used to monitor simultaneously the two orthogonal polarization components. We found the spectral intensity of two wavelengths either increases or decreases synchronously with PCs' tuning. The polarization-resolved spectra at the two orthogonal axes on linear scale (inset is on logarithmic scale) are shown in Fig. 3(a). The corresponding pulse trains are

shown in Fig. 3(b). The polarization-resolved spectra and pulse trains have the same shapes as the ones before polarization resolution. These indicate that the polarization state is the same with the two wavelengths.

Keeping the pump power unchanged and slightly adjusting the PCs, it was noticed that a bright pulse together with a dark pulse could be generated in the fiber laser, which is called bright–dark pulse pair. Fig. 4 shows the spectrum of bright-dark pulse pair. The pulse spectrum contains the same two wavelengths as those of dual-wavelength bright pulse, which resulted from polarization-mode splitting [27]. But there is evidently larger intensity difference between the two wavelengths. The central wavelengths are 1554.8 nm and 1560.9 nm, and the spectral bandwidths are 1.3 nm and 1.4 nm respectively. Fig. 5(a) presents the typical bright–dark pulse train with the fundamental repetition rate on oscilloscope. The depth of the dark pulse is nearly equal to the intensity of the bright pulse in uniform CW background. The bright–dark pulse pair is considerably stable if it has been attained in the experiment. The relative temporal distance between bright and dark pulses could be changed by carefully adjusting the PCs. It is noted that a type of dark soliton in an all-normal dispersion fiber laser has been reported due to an optical domain formation effect, i.e. the formation of the dark soliton is a result of the mutual nonlinear coupling between two different wavelength laser beams [32-34]. Here, we believe the formation mechanism of the bright–dark pulse is mode-locking with the nonlinear couplings between lights with two orthogonal polarizations and two different wavelengths.
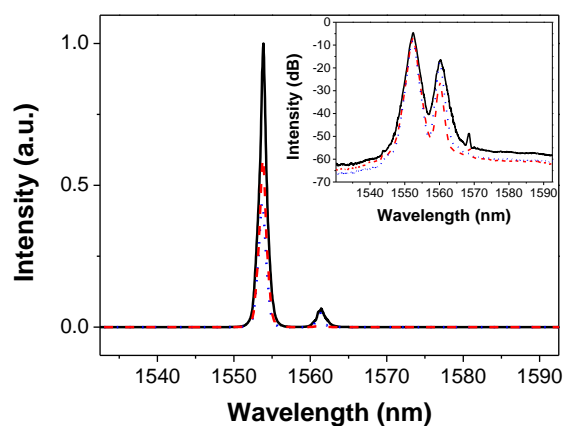

Figure 4 Spectrum of bright-dark pulse pair (black solid line) and its polarization-resolved spectra (red dashed and blue dotted lines) on linear scale (inset is on logarithmic scale).
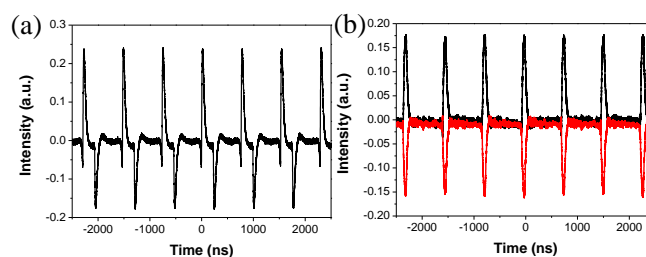

Figure 5 (a) Oscilloscope trace of the bright-dark pulse pair, (b) filtered oscilloscope traces of bright pulse at 1554.8 nm (black curve) and dark pulse at 1560.9 nm (red curve).

The tunable filter was utilized to separate the laser emissions at different wavelengths. When the operation wavelength of the filter was tuned to around 1554.8 nm, only the bright-pulse train appeared on the oscilloscope. Relatively, only the dark-pulse train was observed with the filter adjusted to around 1560.9 nm. Fig. 5(b) displays the filtered bright pulse train at 1554.8 nm and filtered dark pulse train at 1560.9 nm on oscilloscope. Based on this experimental observation, we reckon that the bright–dark pulse pair is combined by two laser beams with different wavebands. The waveband at shorter wavelength corresponds to bright pulse and the waveband at longer wavelength corresponds to dark pulse. The formation and stable propagation of bright–dark pulse pair in the fiber laser is very complicated, mainly due to the nonlinear couplings between lights with two orthogonal polarizations and two different wavelengths [35-37]. The nonlinear couplings include the coupling between two different wavelengths, the coupling between the two orthogonal polarization components of the same beam, and the various combinations of them. In order to understand the real physics behind the observed phenomena, it is necessary to separate the effects first. The further experimental and theoretical are needed. Although the bright and dark pulses are located at different wavelengths, they are bunched together as a unit and propagated stably in the laser cavity, which can be regarded as a group velocity locked pulse pair. Similar to [38, 39], where Guo et al. reported the formation of the bright–dark soliton pair favored by the high nonlinear effect of TI: Bi_2Se_3, we think the cross coupling effect attributes to the bright and dark orthogonal pulse at two wavelength supported by LA-TFBG. Note that the operation wavelengths of the bright–dark pulses may be altered by adjusting the settings of intra-cavity PCs.
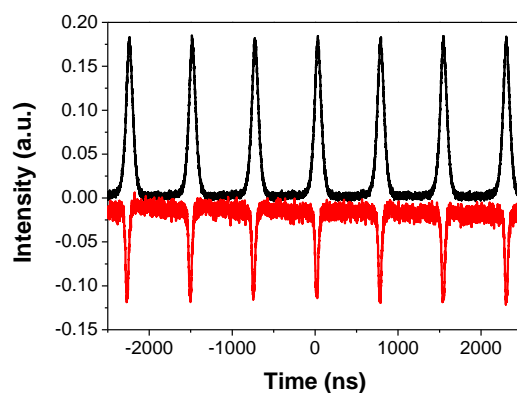

Figure 6 Polarization-resolved oscilloscope traces of the bright-dark pulse pair at two orthogonal axes.

In order to further study the polarization characteristics of the bright–dark pulse pair, the external cavity combiner of PC and PBS was used to observe simultaneously laser emission at two orthogonal polarization axes. By adjusting the external cavity PC to align one of the linear polarization axes of the bright–dark pulses to the vertical or horizontal axis of the PBS, the two orthogonal polarization modes of the pulses can be separated. The polarization-resolved spectra are shown in Fig. 4 (red dashed and blue dotted lines). The corresponding polarization-resolved oscilloscope traces at each port of the PBS are shown in Fig. 6. It is seen that bright and dark pulses with orthogonal polarization states are completely isolated in time domain. While in spectral domain, dark pulse at the longer wavelength has a

strong spectral component with the same polarization at shorter wavelength. We consider it is CW background. Vice versa, bright pulse at the shorter wavelength has a spectral component with the same polarization at longer wavelength. Therefore, we can conclude that the bright and dark pulses within the pulse pair are linearly polarized light with orthogonal electrical vector vibration directions.
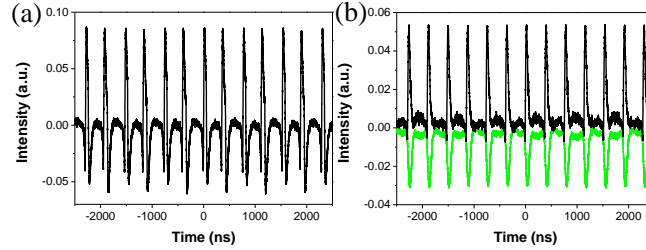

Figure 7 (a) Oscilloscope traces of 2nd harmonic mode-locking of bright-dark pulse pair, (b) its polarization-resolved oscilloscope traces.

When the pump power was increased to 246 mW, the harmonic mode-locking of bright-dark pulse pair could also be obtained by tuning the PCs. Fig. 7(a) shows oscilloscope traces of the 2nd harmonic of bright-dark pulse pair. By further increasing the pump power, 4th or higher order harmonic mode-locking of bright-dark can be attained. Similar to the bright pulse, the harmonic mode-locking of bright-dark pulse pair may be resulted from the interaction between bright-dark pulse pair. Using polarization-resolution method, the harmonic mode-locking of bright-dark pulse pair can also be separated into bright and dark pulses along orthogonal polarization axes, as shown in Fig. 7(b).

3. Conclusions

In conclusion, bright–dark pulse pair with orthogonal polarization has been obtained in a passively mode-locked fiber laser with an LA-TFG. The LA-TFG is employed as polarization-dependent element for mode-locking and two-wavelength filtering induced by polarization-mode splitting. Different from dual-wavelength bright pulses with uniform polarization at two different wavelengths, the bright–dark pulses formed due to the nonlinear coupling between the bright and dark pulses exhibit orthogonal polarization at two different wavebands. Furthermore, harmonic mode-locking of the bright–dark pulse pair has been observed. These pave the way to manipulate the generation of dark pulse in terms of wavelength and polarization with designed LA-TFG, and could find important applications in secure communication system.

References
[1] J. Limpert, F. Roser, T. Schreiber, A. Tunnermann, "High-power ultrafast fiber laser systems," IEEE J. Sel. Top. Quantum Electron. 12, 233 (2006).

[2] B. Oktem, C. Ülgüdür, and F. Ö. Ilday, "Soliton–similariton fibre laser," Nat. Photon. 4, 307 (2010).

[3] P. Grelu and N. Akhmediev, "Dissipative solitons for mode-locked lasers," Nat. Photon. 6, 84 (2012).

[4] Y. S. Kivshar and B. Luther-Davies, "Dark optical solitons: physics and applications," Phys. Rep. 298, 81 (1998).

[5] Hasegawa and F. Tappert, "Transmission of stationary nonlinear optical pulses in dispersive dielectric fibers. II. Normal dispersion," Appl. Phys. Lett. 23, 171 (1973).

[6] M. Weiner, J. P. Heritage, R. J. Hawkins, R. N. Thurston, E. M. Kirschner, D. E. Leaird, and W. J. Tomlinson, "Experimental observation of the fundamental dark soliton in optical fibers ,"Phys. Rev. Lett. 61, 2445 (1988).

[7] Y. S. Kivshar, "Dark-soliton dynamics and shock waves induced by the stimulated Raman effect in optical fibers," Phys. Rev. A 42, 1757 (1990).

[8] D. Tang, J. Guo, Y. Song, H. Zhang, L. Zhao, and D. Shen, "Dark soliton fiber lasers," Opt. Express 22, 19831 (2014).

[9] R. Lin, Y. Wang, P. Yan, J. Zhao, H. Li, S. Huang, G. Cao, and J. Duan, "Bright and dark square pulses generated from a graphene-oxide mode-locked ytterbium-doped fiber laser," Photon. J. IEEE 6, 1500908 (2014).

[10] N. V. Priya, M. Senthilvelan, M Lakshmanan, "Dark solitons, breathers, and rogue wave solutions of the coupled generalized nonlinear Schrödinger equations," Phys. Rev. E 89, 062901 (2014).

[11] V. N. Serkin, A. Hasegawa, "Novel soliton solutions of the nonlinear Schrödinger equation model," Phys. Rev. Lett. 85, 4502 (2000).

[12] V. S. Grigoryan and C. R. Menyuk, "Dispersion-managed solitons at normal average dispersion," Opt. Lett. 23, 609 (1998).

[13] M. Quiroga-Teixeiro, C. B. Clausen, M. P. Srensen, P. L. Christiansen, and P. A. Andrekson, "Passive mode locking by dissipative four-wave mixing," J. Opt. Soc. Amer. B 15, 1315 (1998).

[14] P. Emplit, J. P. Hamaide, F. Reynaud, C. Froehly, and A. Barthelemy, "Picosecond steps and dark pulses through nonlinear single mode fibers," Opt. Commun. 62, 374 (1987).

[15] T. Sylvestre, S. Coen, P. Emplit, and M. Haelterman, "Self-induced modulational instability laser revisited: normal dispersion and dark-pulse train generation," Opt. Lett. 27, 482 (2002).

[16] H. Zhang, D. Y. Tang, L. M. Zhao, and X. Wu, "Dark pulse emission of a fiber laser," Phys. Rev. A 80, 045803 (2009).

[17] Y. F. Song, J. Guo, L. M. Zhao, D. Y. Shen, and D. Y. Tang, "280 GHz dark soliton fiber laser," Opt. Lett. 39, 3484 (2014).

[18] A. Dreischuh, D. N. Neshev, D. E. Petersen, O. Bang, and W. Krolikowski, "Observation of Attraction between Dark Solitons," Phys. Rev. Lett. 96 043901 (2006).

[19] J. P. Tian, H. P. Tian, Z. H. Li, and G. S. Zhou, "Combined solitary-wave solution for coupled higher-order nonlinear Schrödinger equations," J. Opt. Soc. Amer. B 21, 1908 (2004).

[20] X. Li, S. Zhang, Y. Meng, and Y. Hao, "Harmonic mode locking counterparts of darkpulse and dark-bright pulse pairs," Opt. Express, 21, 8409 (2013).

[21] P. Pongwongtragull, C. Teeka, S. Kamoldilok, and P. P. Yupapin, "Novel communication security scheme using dark-bright soliton conversion behaviors," Opt. Eng. 50, 025004 (2011).

[22] Q. Y. Ning, S. K. Wang, A. P. Luo, Z. B. Lin, Z. C. Luo, and W. C. Xu, "Bright–dark pulse pair in a figure-eight dispersion-managed passively mode-locked fiber laser," Photon. J. IEEE 4, 1647 (2012).

[23] C. Mou, H. Wang, B. Bale, K. Zhou, L. Zhang, and I. Bennion, "All-fiber passively mode-locked femtosecond laser using a 45 °-tilted fiber grating polarization element," Opt. Express 18, 18906 (2010).

[24] Z. Zhang, C. Mou, Z. Yan, K. Zhou, L. Zhang, and S. K. Turitsyn, "Sub-100 fs mode-locked erbium-doped fiber laser using a 45 °-tilted fiber grating," Opt. Express 21, 28297 (2013).

[25] J. Albert, L. Shao, and C. Caucheteur, "Tilted fiber Bragg grating sensors," Laser Photon. Rev. 7, 83 (2013).

[26] J. Zheng, X. Dong, P. Zu, L. Y. Shao, C. C. Chan, Y. Cui, and P. Shum, "Magnetic field sensor using tilted fiber grating interacting with magnetic fluid," Opt. Express 21, 17863 (2013).

[27] S. C. Kang, S. Y. Kim, S. B. Lee, S. W. Kwon, S. S. Choi, and B. Lee, "Temperature-independent strain sensor system using a tilted fiber Bragg grating demodulator," IEEE Photon. Technol. Lett. 10, 1461 (1998).

[28] X. Dong, H. Zhang, B. Liu, Y. Miao, "Tilted fiber Bragg gratings: principle and sensing applications," Photon. Sensors 1, 6 (2011).

[29] K. Zhou, L. Zhang, X. Chen, and I. Bennion, "Optic sensors of high refractive-index responsivity and low thermal cross sensitivity that use fiber Bragg gratings of> 80 tilted structures," Opt. Lett. 31, 1193 (2006).

[30] C. Mou, K. Zhou, Z. Yan, H. Fu, and L. Zhang, "Liquid level sensor based on an excessively tilted fibre grating," Opt. Commun. 305, 271 (2013).

[31] Z. Zhang, C. Mou, Z. Yan, Y. Wang, K. Zhou, and L. Zhang, "Switchable dual-wavelength Q-switched and mode-locked fiber lasers using a large-angle tilted fiber grating," Optics Express 23, 1353-1360 (2015).

[32] H. Zhang, D. Tang, L. Zhao, and X. Wu, "Dual-wavelength domain wall solitons in a fiber ring laser," Optics Express 19, 3525 (2011).

[33] C. Lecaplain, P. Grelu, "Dynamics of the transition from polarization disorder to antiphase polarization domains in vector fiber lasers," Phys. Rev. A 89, 63812 (2014).

[34] D. Tang , Y. Song , J. Guo , Y. Xiang , and D. Shen, "Polarization Domain Formation and Domain Dynamics in a Quasi-Isotropic Cavity Fiber Laser," IEEE Journal of Selected Topics in Quantum Electronics 20, 0901309 (2014).

[35] V. B. Afanasjev, E. M. Dianov, and V. N. Serkin, "Nonlinear pairing of short bright and dark solitons by phase cross modulation," IEEE J. Quantum Electron. 25, 2656 (1989).

[36] S. Trillo, S. Wabnitz , E. M. Wright , and G. I. Stegeman, "Optical solitary waves induced by XPM," Optics Letters 13, 871 (1988).

[37] S. Wabnitz, E. M. Wright , and G. I. Stegeman, "Polarization instabilities of dark and bright coupled solitary waves in birefringent optical fibers," Phys. Rev. A 41, 6415 (1990).

[38] B. Guo et al., Observation of Bright-Dark Soliton Pair in a Fiber Laser With Topological Insulator, Photonics Technology Letters 27, 701 (2015).

[39] B. Guo et al.,Topological Insulator-Assisted Dual-Wavelength Fiber Laser Delivering Versatile Pulse Patterns, IEEE J. Sel. Top. in Quantum Electron. 22 (2015).